

# Pressure-induced phase transitions of AX<sub>2</sub>-type iron pnictides: an *ab initio* study

X Wu<sup>1,4</sup>, G Steinle-Neumann<sup>1</sup>, S Qin<sup>2</sup>, M Kanzaki<sup>3</sup> and L Dubrovinsky<sup>1</sup>

<sup>1</sup> Bayerisches Geoinstitut, University of Bayreuth, D-95440 Bayreuth, Germany

<sup>2</sup> Department of Geology, Peking University, Beijing 100871, People's Republic of China

<sup>3</sup> Institute for Study of the Earth's Interior, Okayama University, Misasa, Tottori 682-0193, Japan

E-mail: [xiang.wu@uni-bayreuth.de](mailto:xiang.wu@uni-bayreuth.de)

Received 22 January 2009, in final form 11 March 2009

Published 31 March 2009

Online at [stacks.iop.org/JPhysCM/21/185403](http://stacks.iop.org/JPhysCM/21/185403)

## Abstract

An investigation into the high-pressure behavior of AX<sub>2</sub>-type iron pnictides was conducted using first-principles calculations based on density functional theory within the generalized gradient approximation. Our results demonstrate that a phase transition from the marcasite to the CuAl<sub>2</sub> occurs at 108 GPa for FeP<sub>2</sub>, at 92 GPa for FeAs<sub>2</sub>, and at 38 GPa for FeSb<sub>2</sub>, accompanying a semiconductor-to-metal crossover. A linear relationship between bulk moduli and the inverse specific volume is proposed to be  $B_0 = 17\,498/V_0 - 45.9$  GPa for the marcasite-type phase and  $B_0 = 31\,798/V_0 - 67.5$  GPa for the CuAl<sub>2</sub>-type phase. According to the observed structural evolutions, we claim that the regular marcasite transforms to the CuAl<sub>2</sub>-type phase and the anomalous marcasite transforms to the pyrite-type phase at high pressures.

(Some figures in this article are in colour only in the electronic version)

## 1. Introduction

Since the discovery of high-temperature superconductivity in the iron pnictides with the layered structure where layers of FeAs are separated by spacer layers of LaO [1], the interest in the iron-based superconductor has been growing quickly. Recently the simplest iron pnictide (FeSe) with *P4/nmm* space group has been reported to be a superconductor with  $T_c$  of 8.0 K, which shifts to 27 K at 1.48 GPa [2, 3]. In contrast to metallic properties, AX<sub>2</sub>-type iron pnictides (FeP<sub>2</sub>, FeAs<sub>2</sub> and FeSb<sub>2</sub>) present a semiconductive property with a narrow bandgap, which could be potentially applied to model electronic systems in material physics. At various temperatures and/or pressures a semiconductor-to-metal crossover is reported along with a strong magnetic fluctuation [4–6], which resembles that of FeSi, which is a very important semiconductor. Therefore structural stabilities, electronic and magnetic properties of AX<sub>2</sub>-type iron pnictides at high pressures are also of great theoretical and experimental interest.

At ambient conditions AX<sub>2</sub>-type iron pnictides have a marcasite structure (*Pnmm*,  $Z = 2$ ) with cations at the 2a (0, 0, 0) Wyckoff position and anions at the 4g ( $x, y, 0$ ) position. Each cation has a deformed octahedral environment, and octahedra share edges along the *c* axis (figure 1(A)). A structural study of FeP<sub>2</sub> at high pressures shows that no phase transitions happen up to 28 GPa at room temperature by x-ray diffraction and Raman spectroscopy [7]. However, a distinctive anisotropy of the unit-cell compressibilities was observed in that the shortest *c* axis is the most compressible. The similar high-pressure structural behavior is also reported in FeSb<sub>2</sub> up to 7 GPa at room temperature [8]. As far as we know, no high-pressure structural data are available for FeAs<sub>2</sub>. The AX<sub>2</sub>-type iron pnictides are isostructural with many metal dioxides and dichlorides that undergo a rich series of phase transitions at high pressures, such as from *Pnmm* to *Pbcn*, or to *Pbca*, then to  $Pa\bar{3}$  [9–11]. But an *ab initio* calculation based on the density functional theory (DFT) with local density approximation (LDA) indicates that FeP<sub>2</sub> is unlikely to form those polymorphs at high pressures [7]. Almost ten years ago, a high-pressure polymorph of CrSb<sub>2</sub> was synthesized with the CuAl<sub>2</sub>-type structure (*I4/mcm*,  $Z = 4$ ), in which cations

<sup>4</sup> Author to whom any correspondence should be addressed.

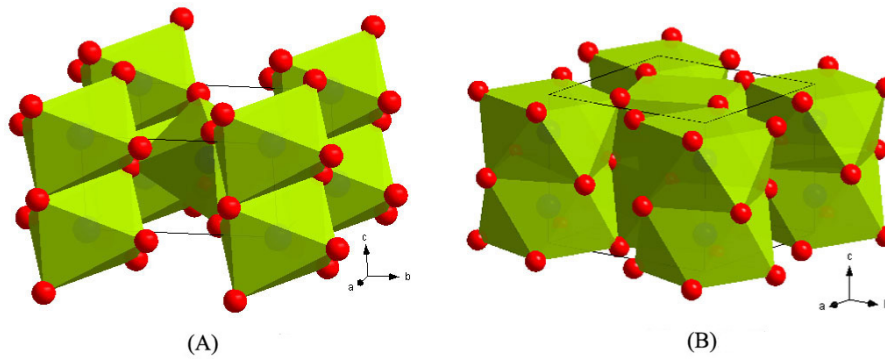


**Figure 1.** The crystal structures of the  $AX_2$ -type iron pnictides with the marcasite phase  $Pnnm$  (A) and the  $CuAl_2$  phase  $I4/mcm$  (B).

occupy the  $4a$   $(0, 0, 0.25)$  Wyckoff position and anions at the  $(x, x+0.5, 0)$  position [12]. Each cation is coordinated by eight anions forming a square antiprism (figure 1(B)), where the bonding character is metallic. Also, the  $CuAl_2$ -type structure was reported in  $TiSb_2$  and  $VSb_2$  compounds [13]. We therefore here expect that the  $AX_2$ -type iron pnictides could crystallize into the  $CuAl_2$ -type polymorph at high pressures.

In the marcasite phase, the ionic configuration of iron is  $d^4$  and its ground state is the low spin state ( $Fe^{4+}t_{2g}^4e_g^0$ ). According to ‘classical’ ligand field theory, the  $Fe$   $t_{2g}$  orbitals are further split into two lower lying orbitals with  $d_{yz}$  and  $d_{xz}$  symmetries and one higher lying orbital with  $d_{xy}$  symmetry [14]. This  $d_{xy}$  state is proposed to play the key role in charge conduction. At ambient conditions, the bandgap of the  $AX_2$ -type iron pnictides is 0.37 eV for  $FeP_2$ , 0.22 eV for  $FeAs_2$  and 0.2 eV for  $FeSb_2$  [15–17]. A theoretical computation indicates that  $FeP_2$  is still a semiconductor at 35 GPa [7], while an experiment on the resistivity in the  $FeSb_2$  compound shows that electrical transport along the  $a$  axis and the  $c$  axis is semiconducting, and the  $b$  axis exhibits a metal–semiconductor crossover at low temperatures [4]. Usually the crossover from a small gap semiconductor to a metallic state occurs at various compositions, temperatures, pressures and magnetic field, such as  $FeSi_{1-x}Ge_x$  at  $x = 0.25$  [18],  $FeS_2$  at 94 GPa [19] and  $FeSi$  at  $\sim 100$  T magnetic field [20]. Here we also expect that this feature exists in the  $AX_2$ -type iron pnictides at high pressures.

In this paper, two polymorphs (the marcasite type and the  $CuAl_2$  type, figure 1) for the  $AX_2$ -type iron pnictides were considered. We investigated their structural stabilities at high pressures by means of the *ab initio* calculation method based on DFT. We computed the equation of state for each phase, as well as the transition pressures between them, provided insights into the atomistic controls on the structural evolutions, and further discussed and summarized the high-pressure behaviors of the  $AX_2$ -type iron pnictides. The rest of this paper is organized as follows: the calculation methods are described in section 2; results and discussion of the structural stabilities under high pressures are presented in section 3; finally a brief conclusion is given in section 4.

## 2. Calculation method

The first-principles calculations performed in this paper are based on the DFT. The total energies have been calculated

within the full potential augmented plane wave (FPAPW) plus the local orbitals (lo) method, implemented in the WIEN2K code [21]. The effects of the approximation to the exchange–correlation energy were treated by the generalized gradient approximation (GGA) [22]. In order to increase the reliability and to obtain a reasonable comparison, we used the same radius of the muffin-tin sphere for the same kind of atoms in all calculations. The muffin-tin radii of Fe, P, As and Sb were chosen as 1.9, 1.7, 1.9 and 2.0 Bohr, respectively. In the LAPW calculations, we set the energy threshold between core and valence states at  $-7.0$  Ryd for the  $FeP_2$  and  $FeAs_2$  and  $-8.0$  Ryd for the  $FeSb_2$ . The muffin-tin radius multiplied by  $K_{max}$  was chosen as 7.0, where  $K_{max}$  is the plane wave cutoff. 1000  $k$ -points were specified in the whole Brillouin zone (BZ). We optimized the  $b/a$  ratio and/or the  $c/a$  ratio for each volume and relaxed all the independent internal atomic coordinates until the forces on every atom were below the value of 1 mRyd/Bohr. For each crystalline phase, we calculated the minimum total energy of the unit cell for a number of different volumes. Finally these energy–volume data were fitted to the third-order Birch–Murnaghan equation of state.

## 3. Results and discussion

The ground-state total energy as a function of the volume for  $AX_2$ -type iron pnictides is given in figure 2. The solid lines are the fits of the calculation data using the Birch–Murnaghan equation of state. Figure 2 clearly shows that a phase transition of the  $AX_2$ -type iron pnictides occurs from  $Pnnm$  to  $I4/mcm$ . According to the different Gibbs free energy as a function of pressure (the inset of figure 2), the transition pressures are 108 GPa, 92 GPa and 38 GPa for  $FeP_2$ ,  $FeAs_2$ , and  $FeSb_2$ , respectively. The corresponding volume collapses at the phase-transition boundaries were also calculated as 4.3%, 3.6% and 4.7%, respectively. The theoretical ground-state parameters ( $V_0$ ,  $B_0$  and  $B'_0$ ) are listed in table 1 and compared with the available data. The calculated  $V_0$  values are consistent with those of the experiments. The relative error is about 1%, that is the typical precision of GGA-DFT calculations. The bulk modulus of the marcasite-type  $FeP_2$  has been measured to be about 235(3) GPa [7], which is larger than our theoretical result (178 GPa). The higher  $B_0$  in that experiment are possibly

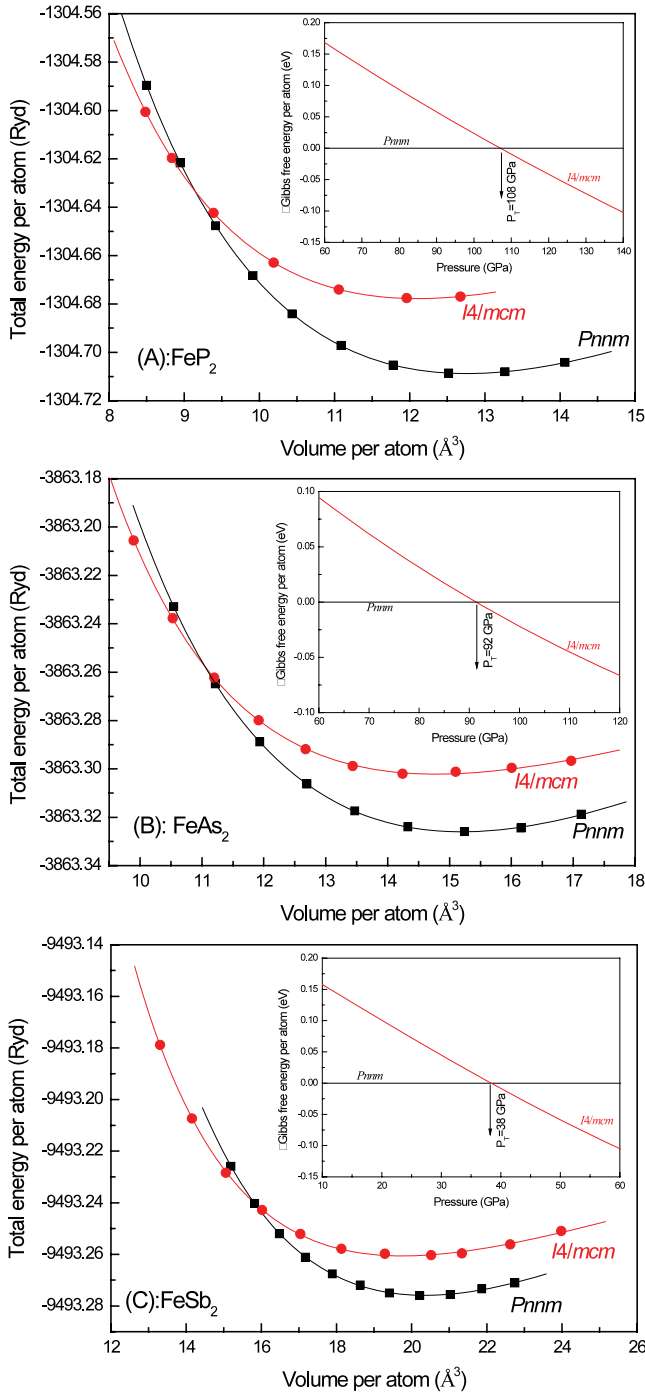


**Figure 2.** Calculation of the total energy versus volume for the AX<sub>2</sub>-type iron pnictides with the marcasite phase and the CuAl<sub>2</sub> phase. (A): FeP<sub>2</sub>; (B): FeAs<sub>2</sub>; (C): FeSb<sub>2</sub>. The inset: calculated different Gibbs free energy versus pressure for all compounds. The corresponding phase-transition pressure is marked.

attributed to a large pressure gradient using an LiF pressure-transmitting medium and conventional x-ray source, while the bulk modulus of the marcasite-type FeSb<sub>2</sub> is in good agreement with the experimental result using monochromatic synchrotron x-rays and liquid pressure-transmitting medium [8]. For AX<sub>2</sub>-type iron pnictides, the  $B_0$  of the marcasite phase is larger than that of the CuAl<sub>2</sub> phase and their  $B_0$  decreases with the larger

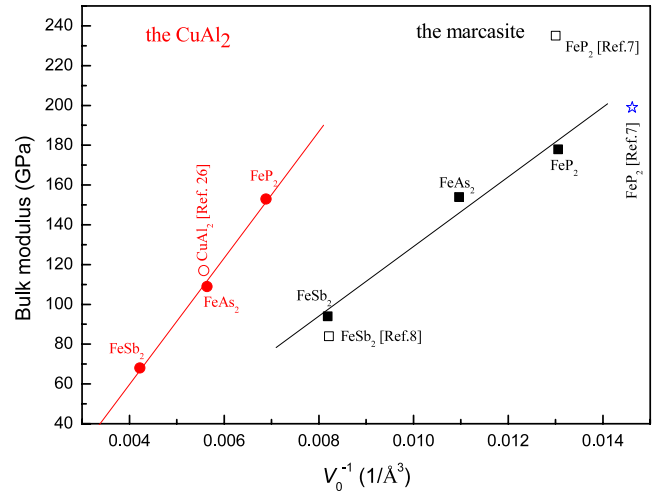


**Figure 3.** Bulk moduli ( $B_0$ ) of the AX<sub>2</sub>-type compounds plotted as a function of inverse volume ( $1/V_0$ ). The solid symbols are our present data, the open symbols are from x-ray diffraction experimental results [7, 8, 26] and the star symbol is from the LDA-DFT calculation [7].

**Table 1.** Equation-of-state parameters of the AX<sub>2</sub>-type iron pnictides obtained from experiments and computations.  $V_0$  is the value of the unit-cell volume at 0 GPa,  $B_0$  is the bulk modulus and  $B'_0$  is its pressure derivative.

AX <sub>2</sub>	Phase	Method	$V_0$ (Å <sup>3</sup> )	$B_0$ (GPa)	$B'_0$	
FeP <sub>2</sub>	<i>Pnmm</i>	GGA	76.6	178	4.3	
		LDA [7]	68.4	199	4.4	
		Exp [7]	76.88(6)	235(3)	4	
FeAs <sub>2</sub>	<i>I4/mcm</i>	GGA	145.2	153	5.0	
		<i>Pnmm</i>	GGA	91.2	154	4.1
		Exp [16]	91.38			
FeSb <sub>2</sub>	<i>I4/mcm</i>	GGA	177.4	109	5.5	
		<i>Pnmm</i>	GGA	122.1	94	4.9
			Exp [8]	121.7	84(3)	5(1)
	<i>I4/mcm</i>	GGA	237.0	68	5.9	

anionic radius. Generally the relationship between bulk moduli and specific volume is linear, i.e.  $B \times V = \text{constant}$ , for simple oxide structures in the absence of phase transitions [23, 24]. Here we also figured out the bulk modulus of the AX<sub>2</sub>-type iron pnictides as a function of inverse spatial volume (figure 3). A linear trend of  $B_0 = 17498/V_0 - 45.9$  GPa was obtained for the marcasite-type phase, and  $B_0 = 31798/V_0 - 67.5$  GPa for the CuAl<sub>2</sub>-type phase. According to the trend, the bulk modulus of the CuAl<sub>2</sub> ( $V_0 = 179.09$  Å<sup>3</sup> [25]) is predicted to be 110 GPa, in excellent agreement with  $B_0 = 117$  GPa determined by Grin *et al* [26] from *in situ* x-ray diffraction measurements. Thus the bulk moduli of the analogs can be roughly predicted if we know their volumes in the marcasite-type and/or the CuAl<sub>2</sub>-type phases, such as NiAs<sub>2</sub> and CrSb<sub>2</sub>.

In order to better understand the high-pressure structural behavior, axial compressibilities of the marcasite-type and the CuAl<sub>2</sub>-type phases were described by a linear version of the Murnaghan EoS, where  $d_0$  is the value of the unit-cell axis at room pressure,  $B_d$  is the compressional modulus of the axis and  $B'_d$  is its pressure derivative. Table 2 lists all parameters

**Table 2.** The parameters of the axial compressibilities.

AX <sub>2</sub>	Phase	Axis	d <sub>0</sub> (Å)	B <sub>d</sub> (GPa)	B' <sub>d</sub>
FeP <sub>2</sub>	<i>Pnnm</i>	<i>a</i>	4.940	242	4.7
		<i>b</i>	5.647	194	5.1
		<i>c</i>	2.755	128	3.6
	<i>I4/mcm</i>	<i>a</i>	5.351	191	3.8
		<i>c</i>	5.003	208	4.0
FeAs <sub>2</sub>	<i>Pnnm</i>	<i>a</i>	5.287	209	4.0
		<i>b</i>	5.986	162	4.8
		<i>c</i>	2.884	110	3.7
	<i>I4/mcm</i>	<i>a</i>	5.695	186	4.0
		<i>c</i>	5.387	129	4.0
FeSb <sub>2</sub>	<i>Pnnm</i>	<i>a</i>	5.841	133	4.0
		<i>b</i>	6.528	124	4.1
		<i>c</i>	3.191	76	3.6
	<i>I4/mcm</i>	<i>a</i>	6.344	108	4.0
		<i>c</i>	5.720	109	4.0

of axial compressibilities. For the marcasite-type phase, the compressibility of the *a* axis is the least compressible and the *c* axis is the most compressible. The *B<sub>a</sub>/B<sub>c</sub>* ratio is close to 1.9, which is consistent with the experimental result of 2.2 [7]. In the CuAl<sub>2</sub>-type phase, the compressibilities of the *a* axis and the *c* axis are similar, which agrees with those of the isostructural TiSb<sub>2</sub> [13] and CuAl<sub>2</sub> [26]. As we know, iron atoms lie in the deformed octahedral environment in the marcasite phase and are surrounded by eight pnictogen atoms, forming a square antiprism in the CuAl<sub>2</sub> phase. In both phases, the internal coordinates of cations are fixed by symmetry, and only those of anions can shift at high pressure. This degree of freedom results in a significant change of the iron–pnictogen ligands. Figure 4 displays the iron–pnictogen and the iron–iron bond lengths at various pressures. In the marcasite phase, the divergent trend of the iron–pnictogen bond lengths in the octahedral environments (figure 4(A)) indicates that pressure enhances the structural distortion. At the boundary of the phase transition (the *Pnnm* to *I4/mcm*), the increase of the iron–pnictogen distance is about 0.12 Å, in good agreement with the increase (0.14 Å) obtained from the ionic radii of Fe<sup>2+</sup> between sixfold and eightfold [27]. However there is a collapse of the iron–iron bond length at the boundary of the phase transition (figure 4(B)). The change of the above bond lengths indicates a transition of the bonding character from mixed ionic and covalent to metallic.

As we know, the AX<sub>2</sub>-type iron pnictides with the marcasite-type phase are semiconductors with quite a low bandgap. At 0 GPa the direct energy bandgaps in our calculations are 0.40 eV for FeP<sub>2</sub>, 0.25 eV for FeAs<sub>2</sub> and 0.20 eV for FeSb<sub>2</sub>, which are consistent with previous results [15–17] (0.37, 0.22 and 0.2 eV, correspondingly). Figure 5 displays the energy bandgaps of the marcasite-type phases at various pressures. At the beginning, the bandgaps of all iron pnictides present a positive pressure shift, then at higher pressures the pressure shifts of the gaps become negative (figure 5). Especially in the FeSb<sub>2</sub> case, a small density of states crosses the Fermi level at *P* > 10 GPa, indicating that it presents a weak metallic property. An obvious semiconductor-to-metal crossover occurs when the marcasite phase transforms to the CuAl<sub>2</sub> phase (figure 6).

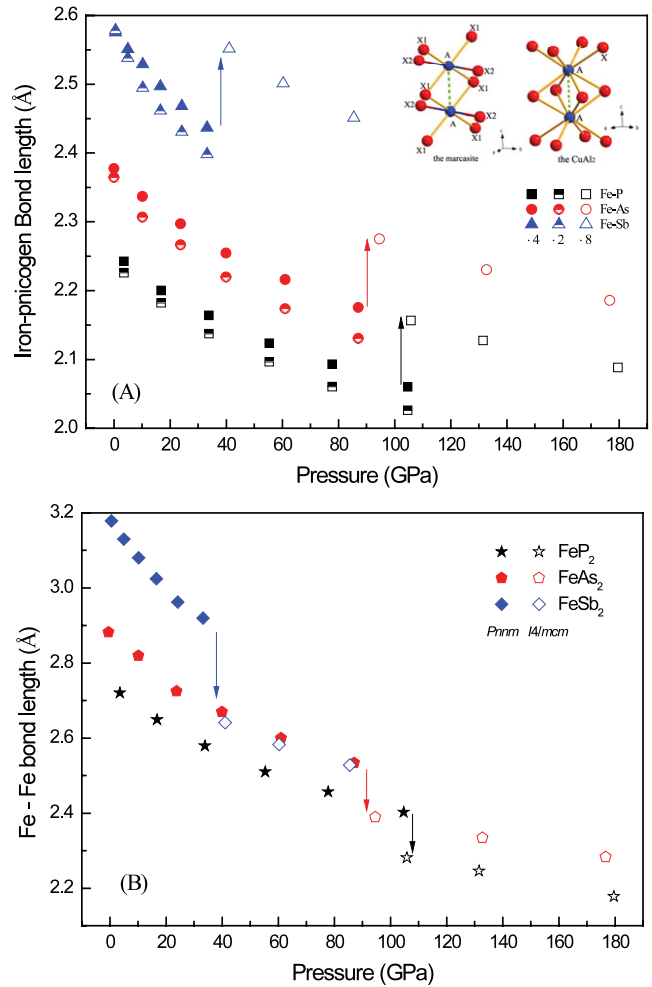


**Figure 4.** The iron–pnictogen bond lengths (A) and the iron–iron bond lengths (B) of the AX<sub>2</sub>-type iron pnictides at various pressures. The solid and the half-open symbols are for the marcasite-type phase, and the open symbols are for the CuAl<sub>2</sub>-type phase. Fragments of both the marcasite-type structure and the CuAl<sub>2</sub>-type structure are displayed in the inset of (A). Iron or pnictogen atoms have crystallographically equivalent positions, but they are labeled by individual names for the sake of description. In the octahedral environment, there are four long iron–pnictogen bond distances (A–X1) and two short bond distances (A–X2), while the eight iron–pnictogen bond lengths (A–X) are the same in the square-antiprism environment.

At various temperatures and/or pressure conditions the marcasite-type compounds have a number of different polymorphs. Like our above results, the iron pnictides can form the CuAl<sub>2</sub>-type phase at high pressures. Both the pyrite and the marcasite phases were observed in FeS<sub>2</sub> [28]. Marcasite-type NiAs<sub>2</sub> transforms into the pararammelsbergite-type phase at 853 K [29], and a high-pressure pyrite-type phase of NiP<sub>2</sub> has been synthesized [30]. The present literature shows that the marcasite-type compounds have two kinds of phase-transition paths at high pressures: the marcasite-to-pyrite (pararammelsbergite-type and arsenopyrite-type as possible intermediate structures) and the marcasite-to-CuAl<sub>2</sub>. In order to better reveal the reason for different structural behaviors, we here review the marcasite structure in detail. Usually the

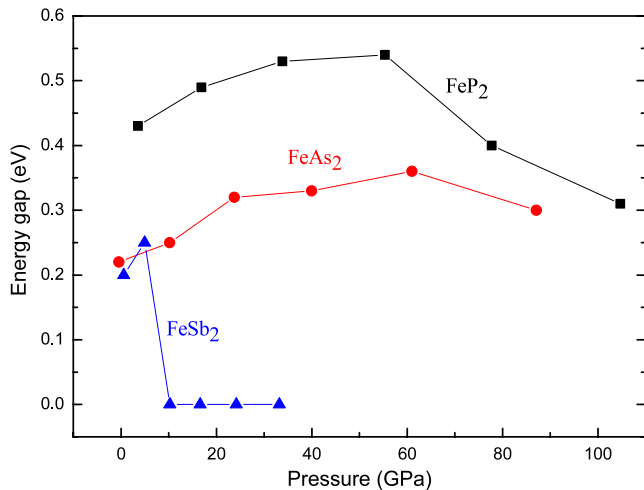


**Figure 5.** The energy bandgap of the marcasite-type phase versus pressure.

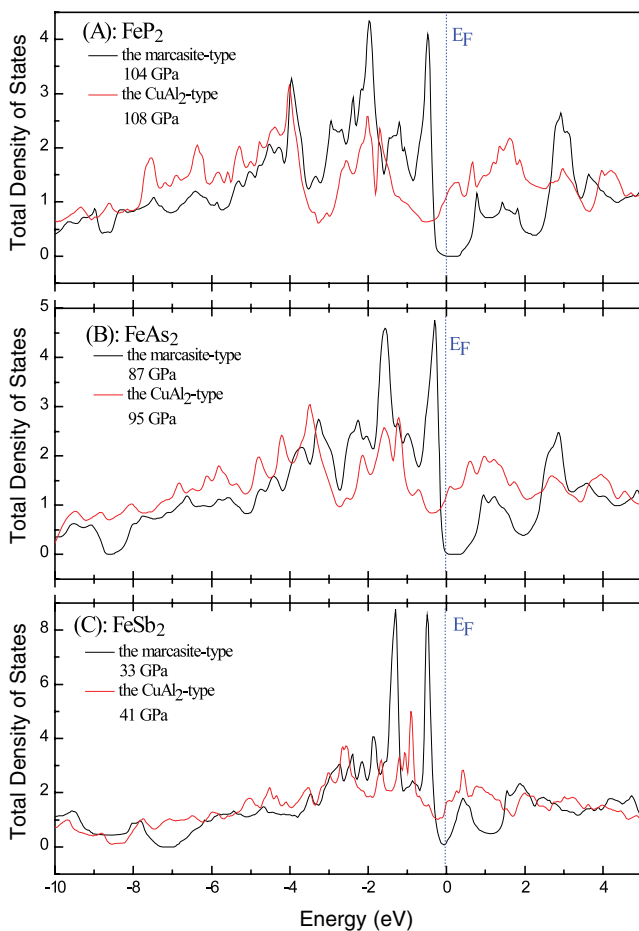


**Figure 6.** Total density of states of the AX<sub>2</sub>-type iron pnictides with the marcasite and the CuAl<sub>2</sub> structures. (A) FeP<sub>2</sub>, (B) FeAs<sub>2</sub> and (C) FeSb<sub>2</sub>.

marcasite structures are classified into ‘anomalous marcasite’ and ‘regular marcasite’ according to the  $c/a$  ratio, cation  $d$ -electron configuration and the A–X1–A bond angle  $\alpha$  (the inset of figure 4) between the neighboring cations in edge-sharing

octahedra along the  $c$  axis [31]. The regular marcasite has a small  $c/a$  ratio of 0.53–0.57, a  $d^n$  configuration with  $n \leq 4$  for cations and  $\alpha < 90^\circ$ , while the anomalous marcasite has a large  $c/a$  ratio of 0.73–0.75, a  $d^n$  configuration with  $n \geq 6$  for cations and  $\alpha > 90^\circ$ . Thus FeP<sub>2</sub>, FeAs<sub>2</sub>, FeSb<sub>2</sub>, CrSb<sub>2</sub>, etc, are classified as the regular marcasite. FeS<sub>2</sub>, FeSe<sub>2</sub>, FeTe<sub>2</sub>, NiP<sub>2</sub>, etc, belong to the anomalous marcasite. For the regular marcasite, the shortest  $c$  axis with the most compressibility and the  $\alpha$  deviation from  $90^\circ$  at high pressures [7, 8] lead to more deformed AX<sub>6</sub> octahedra and a shorter distance of A–A bond length, which results in a transition to the CuAl<sub>2</sub>-type structure with metallic property. However, for the anomalous marcasite, the shortest  $c$  axis becomes the least compressible, and the  $\alpha$  decreases towards  $90^\circ$  [9], which results in a transition to the pyrite-type structure with an effective packing of AX<sub>6</sub> octahedra.

#### 4. Conclusion

In conclusion, *ab initio* calculations based on DFT within the GGA present a phase transition of the AX<sub>2</sub>-type iron pnictides from the marcasite to the CuAl<sub>2</sub>, accompanying a semiconductor-to-metal crossover. The phase-transition pressure decreases with the increase of the pnictogen ionic radius. A linear relationship between bulk moduli and inverse specific volume is proposed to be  $B_0 = 17\,498/V_0 - 45.9$  GPa for the marcasite-type phase and  $B_0 = 31\,798/V_0 - 67.5$  GPa for the CuAl<sub>2</sub>-type phase. The marcasite-type structure presents a distinctive anisotropy in that the shortest  $c$  axis is the most compressible. However, an almost isotropy of the axial compressibility appears in the CuAl<sub>2</sub>-type phase. Finally, from the observed structural evolutions we may claim that the regular marcasite transforms to the AuAl<sub>2</sub>-type phase and the anomalous marcasite transforms to the pyrite-type phase at high pressures.

#### Acknowledgments

XW is grateful for his Alexander von Humboldt Fellowship. SQ acknowledges the financial support of the National Natural Science Foundation of China (grant no. 40672024).

#### References

- [1] Kamihara Y, Watanabe T, Hirano M and Hosono H 2008 *J. Am. Chem. Soc.* **130** 3296
- [2] Hsu F C, Luo J Y, Yeh K W, Chen T K, Huang T W, Wu P M, Lee Y C, Huang Y L, Chu Y Y, Yan D C and Wu M K 2008 *Proc. Natl Acad. Sci. USA* **105** 14262
- [3] Mizuguchi Y, Tomioka F, Tsuda S, Yamaguchi T and Takano Y 2008 arXiv:0807.4315
- [4] Petrovic C, Kim J W, Bud’ko S L, Goldman A I, Canfield P C, Choe W and Miller G J 2003 *Phys. Rev. B* **67** 155205
- [5] Perucchi A, Degiorgi L, Hu R, Petrovic C and Mitrović V F 2006 *Eur. Phys. J. B* **54** 175
- [6] Lukoyanov A V, Mazurenko V V, Anisimov V I, Sigrist M and Rice T M 2006 *Eur. Phys. J. B* **53** 205
- [7] Wu X, Kanzaki M, Qin S, Steinle-Neumann G and Dubrovinsky L 2009 *High Pressure Res.* at press

- [8] Petrovic C, Lee Y, Vogt T, Lazarov N D, Bud'ko S L and Canfield P C 2005 *Phys. Rev. B* **72** 045103
- [9] Wu X and Wu Z Y 2006 *Eur. Phys. J. B* **50** 521
- [10] Ono S, Tsuchiya T, Hirose K and Ohishi Y 2003 *Phys. Rev. B* **68** 134108
- [11] Hugosson H W, Grechnev G E, Ahuja R, Helmersson U, Sa L and Eriksson O 2002 *Phys. Rev. B* **66** 174111
- [12] Takizawa H, Uheda K and Endo T 1999 *J. Alloys Compounds* **287** 145
- [13] Armbrüster M, Schnelle W, Schwarz U and Grin Y 2007 *Inorg. Chem.* **46** 6319
- [14] Goodenough J B 1972 *J. Solid State Chem.* **5** 144
- [15] Boda G, Stenstrom B, Sagredo V, Beckman O, Carlsson B and Rundqvist S 1971 *Phys. Scr.* **4** 132
- [16] Fan A K L, Rosenthal G H, McKinzie H L and Wold A 1972 *J. Solid State Chem.* **5** 136
- [17] Bentien A, Madsen G K H, Johnsen S and Iversen B B 2006 *Phys. Rev. B* **74** 205105
- [18] Tsujii N, Yamaokab H, Oohashic H, Jarrigid I, Nomotoe D, Takahirof K, Ozakif K and Kawatsuraf K 2008 *Physica B* **403** 922
- [19] Cai J, Goliney I and Philpott M R 2006 *J. Phys.: Condens. Matter* **18** 9151
- [20] Anisimov V I, Ezhov S Y, Elfimov I S, Solovyev I V and Rice T M 1996 *Phys. Rev. Lett.* **76** 1735
- [21] Blaha P, Schwarz K, Madsen G K H, Kvasnicka D and Luitz J 2002 *WIEN2k, An Augmented Plane Wave-Local Orbitals Program for Calculating Crystal Properties* revised edition June 2002, Univ Prof. Dr. Karlheinz Schwarz Technische Universität Wien, Institut für Physikalische und Theoretische Chemie, Getreidemarkt 9/156 A-1060Wien/Austria
- [22] Perdew J P, Burke S and Ernzerhof M 1996 *Phys. Rev. Lett.* **77** 3865
- [23] Anderson O L and Nafe J E 1965 *J. Geophys. Res.* **70** 3951
- [24] Ross N L and Chaplin T D 2003 *J. Solid State Chem.* **172** 123
- [25] Havinga E E, Damsma H and Hokkeling P 1972 *J. Less-Common Met.* **27** 169
- [26] Grin Y, Wagner F R, Armbrüster M, Kohout M, Leithe-Jasper A, Schwarz U, Wedig U and Schnering H G 2006 *J. Solid State Chem.* **179** 1707
- [27] Shannon R D 1976 *Acta Crystallogr. A* **32** 751
- [28] Rieder M, Crelling J C, Sustai O, Drabek M, Weiss Z and Klementova M 2007 *Int. J. Coal Geol.* **71** 115
- [29] Kjekshus A and Rakke T 1979 *Acta Chem. Scand. A* **33** 609
- [30] Donohue P C, Bither T A and Young H S 1968 *Inorg. Chem.* **7** 998
- [31] Hulliger F and Mooser E 1965 *J. Phys. Chem. Solids* **26** 429